Why Does Wurtzite Form in Nanowires of III-V Zinc Blende Semiconductors?

Frank Glas,* Jean-Christophe Harmand, and Gilles Patriarche
CNRS-Laboratoire de Photonique et de Nanostructures, route de Nozay, 91460 Marcoussis, France

(Received 30 May 2007; published 5 October 2007)

We develop a nucleation-based model to explain the formation of the wurtzite phase during the catalyzed growth of freestanding nanowires of zinc blende semiconductors. We show that in vapor-liquid-solid nanowire growth, nucleation generally occurs preferentially at the triple phase line. This entails major differences between zinc blende and wurtzite nuclei. Depending on the pertinent interface energies, wurtzite nucleation is favored at high liquid supersaturation. This explains our systematic observation of zinc blende during early growth of gold-catalyzed GaAs nanowires.

DOI: 10.1103/PhysRevLett.99.146101 PACS numbers: 68.65.La, 64.60.Qb, 64.70.Nd, 81.15.Kk

Free-standing wires with diameters ranging from hundreds down to a few nanometers are nowadays commonly fabricated from a large range of semiconductor materials [1–5]. These nanowires have remarkable physical properties and many potential applications. The present Letter deals with the epitaxial growth of nanowires of III–V semiconductors on a hot substrate. Metal catalyst nanoparticles deposited on the substrate before growth define the wire diameter. According to the vapor-liquid-solid growth mechanism, the atoms are fed from the vapor phase to the solid wire through this particle (or droplet), which remains liquid during growth [6].

We consider III–V compounds which, under bulk form, adopt the cubic zinc blende (ZB) crystal structure [7] (although some of their non-ZB high-pressure phases [8] may be metastable at atmospheric pressure [9]). We discuss the usual case of nanowires grown on a (111)B (As-terminated) face of the ZB substrate. Probably the most surprising feature of these nanowires is that, in contrast to their bulk counterparts, they often adopt the hexagonal wurtzite (WZ) structure. This has been observed for most ZB III–V materials and growth techniques [1,3,4,10,11]. However, although often dominantly of WZ structure, the nanowires usually contain stacking faults and sequences of ZB structure. Since the coexistence of two phases impedes basic studies as well as applications, phase purity control is one of the main challenges of III–V nanowire fabrication.

The surprising prevalence of the WZ structure in III–V nanowires has not been explained satisfactorily so far. Here, based on new experimental observations, we propose an explanation of the occurrence of the WZ structure and develop a model predicting quantitatively for which materials and in which growth conditions it should form. We consider the specific case of gold-catalyzed GaAs nanowires grown by molecular beam epitaxy (MBE) on a GaAs substrate. However, we expect our model and our criteria for WZ formation to apply to any ZB III–V compound and any growth method.

The difference δw in cohesive energy between ZB and WZ bulk GaAs is about 24 meV per III–V pair [7]. It has been argued that this favoring of the ZB structure might be offset in nanowires of small diameter by the large relative contribution to the total energy of either the lateral facets [12] or the vertical edges separating facets [13] (provided the specific energies of these features are less for WZ than for ZB). This leads to critical radii under which WZ wires should be more stable than ZB wires. These approaches have in common to treat the energetics of *fully formed* wires and to predict critical radii far too small (e.g., 5.6 nm for GaAs [13]) to explain the occurrence of WZ in wires with radii as large as 100 nm.

Moreover, the standard theories of nanowire growth are based on nucleation [14–17], and experiments suggest that, once a nucleus of critical size forms at the solid-liquid interface, it rapidly spreads out laterally over the whole interface [5,11], unless the wire is very wide [16]. In the present Letter, we shall thus search the reason for the formation of the WZ phase in the preferential formation of WZ nuclei at the solid-liquid interface.

Given the prominence of WZ in GaAs nanowires, it is interesting to find two instances where ZB *systematically* appears in our nanowires. The first one corresponds to the initial stage of growth. By growing GaAs nanowires for short times, we ensured that the foot of each wire could be observed clearly before being buried by the 2D layer which grows concomitantly albeit more slowly between the wires. The cross-sectional images obtained *ex situ* by transmission electron microscopy (TEM) prove that the whole nanowire is initially pure ZB. Growth then switches abruptly to WZ stacking (Fig. 1). Scanning electron microscopy shows that, at this early stage, the wires are actually pyramids with triangular bases and tilted lateral facets. These facets become vertical at the ZB → WZ transition (Fig. 1).

Second, when we terminate MBE growth by switching off the Ga flux while maintaining an As flux, we systematically observe a section of nanowire that adopts the ZB structure. This effect, already reported for GaAs wires grown by chemical beam epitaxy [3], is interpreted as a partial consumption of the Ga dissolved in the gold particle to form the terminal section of the nanowire.

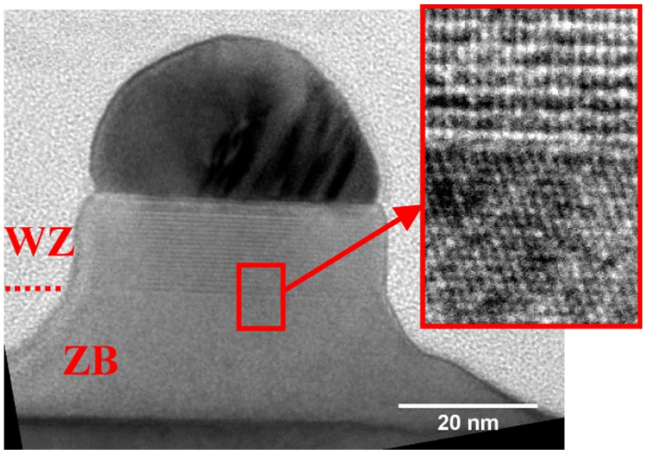

FIG. 1 (color online). Transmission electron microscopy image of a short GaAs nanowire with high resolution close-up of the transition zone between zinc blende and wurtzite phases.

These two situations where ZB forms have in common to be transient growth phases during which the supersaturation of Ga (and possibly As) in the liquid is less than during steady wire growth. Before growth, the deposited Au droplets dissolve the substrate locally to achieve equilibrium with it: the supersaturation is zero. When vapor fluxes are turned on, the supersaturation increases until a permanent regime settles. Symmetrically, during growth termination, the Ga concentration in the droplet, and hence supersaturation, decrease, since the atoms used to build the nanowire are not replaced. This strongly suggests that ZB systematically forms when the supersaturation is less than some critical value and, conversely, that WZ formation requires a *high supersaturation*.

Since critical nucleus sizes and nucleation energy barriers scale inversely with supersaturation, our observations point to a preferential formation of WZ when the critical nuclei are small. This recalls the preference for WZ of nanowires of small radius [12,13], but we cannot simply assume it to apply to nuclei. Instead, we should compare the probabilities of forming various nuclei from the liquid phase. As a first approximation, we shall simply compare their formation energies, which largely determine these probabilities [18]. In order not to obscure our demonstration, we keep as far as possible to classical nucleation theory [18], resorting to an atomistic picture only when necessary. We proceed in two stages. We first show that nucleation must occur at the edge of the solid-liquid interface (the vapor-liquid-solid *triple phase line*), rather than elsewhere in this interface. We then show that, at the triple phase line, the formation of WZ nuclei is favored over that of ZB nuclei, provided certain conditions about material and supersaturation are met.

Let us consider the interface between a nanowire (hereafter called substrate) and the liquid droplet. There, the formation, from the liquid phase, of a solid epitaxial 2D island of height h (1 monolayer of III–V pairs), *entirely surrounded by the liquid* along its lateral side (perimeter length P) and upper surface (area A) [Fig. 2(a)], involves a change of free enthalpy:

$$\Delta G = -\mathrm{Ah}\Delta\mu + \mathrm{Ph}\gamma_{\ell L} + A(\gamma_{\mathrm{NL}} - \gamma_{\mathrm{SL}} + \gamma_{\mathrm{SN}}) \quad (1)$$

In Eq. (1), $\Delta\mu > 0$ is the difference of chemical potential for III–V pairs between liquid and solid phases, per unit volume of nucleus; $\gamma_{\ell L}$ is the energy per unit area of the *lateral* interface between nucleus and liquid; γ_{SL}, γ_{SN}, and γ_{NL} are, respectively, the energies per unit area of the substrate-liquid, substrate-nucleus and upper nucleus-liquid interfaces [Fig. 2(a)]. Note that all interface energies may depend on growth conditions.

A given nucleus (set of atoms with fixed relative positions) of monolayer height cannot be said to be of ZB or WZ structure. It is only the *orientational positioning* of the nucleus with respect to the previous monolayer which determines if the stack of 2 monolayers formed by adding the nucleus is of the type found in ZB or WZ crystals (Fig. 3). In the former case (hereafter "ZB position"), the GaAs_4 tetrahedra have the same orientation in the nucleus and in the previous monolayer whereas they are rotated by an odd multiple of $\pi/3$ in the latter case ("WZ position") [7]. Note that ZB and WZ *sequences* require the nucleation of *each* monolayer in, respectively, ZB and WZ positions with respect to the previous monolayer.

Whatever the nucleus position, the interfaces between solid or upper nucleus and liquid have the same atomic configuration (Fig. 3) so that $\gamma_{\mathrm{SL}} = \gamma_{\mathrm{NL}}$. Moreover, since we consider a given nucleus with given edges, $\gamma_{\ell L}$ is the same in ZB and WZ positions. On the other hand, nucleation in WZ position costs some substrate-nucleus interfacial energy ($\gamma_{\mathrm{SN}}^{\mathrm{WZ}} = \gamma_F$) whereas nucleation in ZB position does not ($\gamma_{\mathrm{SN}}^{\mathrm{ZB}} = 0$). Hence, from Eq. (1), the formation enthalpies of the nucleus in ZB or WZ position are $\Delta G^{\mathrm{ZB,WZ}} = -\mathrm{Ah}\Delta\mu + \mathrm{Ph}\gamma_{\ell L} + A\gamma_{\mathrm{SN}}^{\mathrm{ZB,WZ}}$. Since $\Delta G^{\mathrm{WZ}} - \Delta G^{\mathrm{ZB}} = A\gamma_F > 0$, nucleation *away from the triple phase line* occurs preferentially in ZB position.

We now show that nucleation should take place at the triple phase line. To this end, we compare the formation of a given nucleus at two different locations (Fig. 2): its lateral surface is either entirely surrounded by the liquid, as assumed above (1) or partly surrounded by the vapor

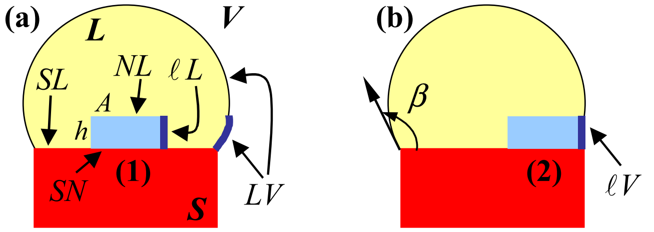

FIG. 2 (color online). (a) Nucleus at the nanowire-liquid interface, with interfaces of interest. (b) Transferring the nucleus to the triple phase line eliminates and creates interfacial areas, indicated by thick lines in, respectively, (a) and (b). For explanation of the symbols, see text.

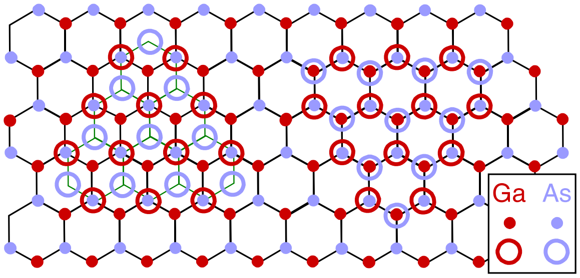

FIG. 3 (color online). A given nucleus (open symbols) in ZB (left) and WZ (right) positions on top of a (111)B monolayer (disks).

because of nucleation at the triple phase line (2). We now have to distinguish the specific energies $\gamma_{\ell L}$ and $\gamma_{\ell V}$ of the lateral nucleus-liquid and nucleus-vapor interfaces. The key point is that shifting the nucleus from location (1) to location (2) *at constant liquid volume* has a major effect: it eliminates part of the liquid-vapor interface and replaces it by a nucleus-vapor interface (Fig. 2). Suppose that forming an area s of the latter interface eliminates an area τs of liquid-vapor interface, of energy $\gamma_{\rm LV}$. If α is the fraction of the island perimeter in contact with the vapor, the formation enthalpy of the nucleus is

$$\Delta G(\alpha) = -\mathrm{Ah}\Delta\mu + \mathrm{Ph}[(1-\alpha)\gamma_{\ell L} + \alpha(\gamma_{\ell V} - \tau\gamma_{\rm LV})] + A\gamma_{\rm SN} \qquad (2)$$

where, as above, $\gamma_{\rm SN} = 0$ or γ_F for, respectively, ZB or WZ nuclei. *For a given nucleus*, the difference in formation enthalpies between locations (1) and (2) is $\Delta G(\alpha) - \Delta G(0) = \alpha\mathrm{Ph}(\gamma_{\ell V} - \gamma_{\ell L} - \tau\gamma_{\rm LV})$. Since factor τ cannot be calculated exactly, we estimate it by considering an artificially axisymmetric nucleus. This readily yields $\tau = \sin\beta$, with β the contact angle between droplet and wire (Fig. 2).

Hence, a given nucleus tends to form at the triple phase line provided $\gamma_{\ell V} - \gamma_{\ell L} - \gamma_{\rm LV}\sin\beta < 0$. Let us examine if this inequality is satisfied. Before growth, we measure by TEM contact angles between our liquid droplets and planar bulk GaAs close to $\pi/2$, which implies (from Young's equation) that the solid-liquid and solid-vapor interface energies are close for (111)B surfaces. Assuming that this also holds for the lateral nucleus faces yields $\gamma_{\ell L} \simeq \gamma_{\ell V}$. In turn, $\gamma_{\rm LV}$ should lie between the surface energies of pure liquid Au and Ga (1.14 and 0.72 $\mathrm{J\cdot m^{-2}}$ [19]). After growth, in all our samples, $90° \leq \beta \leq 125°$, so that $\sin\beta \geq 0.82$. Hence, the above inequality is safely satisfied, and the critical nuclei should always form at the triple phase line. This remains true for appreciably different $\gamma_{\ell L}$ and $\gamma_{\ell V}$ and for larger contact angles. In essence, forming the nucleus there is favorable because it eliminates a portion of the *preexisting* droplet surface; this largely outweighs the replacement of part of the lateral nucleus-liquid interface by a possibly slightly costlier nucleus-vapor interface. Nucleation at the triple phase line in GaP nanowires has previously been argued for on an entirely different basis, namely, the low solubility of phosphorus in gold [5]. Our argument is of general validity and would even apply to solid catalyst particles [3].

We now have to demonstrate the advantage of WZ over ZB nucleation *at the triple phase line* for each successive monolayer. To this end, we consider the atomic structure of the top facet of the nanowire and of the nucleus, restricting ourselves to low energy configurations with at most one nonvertical dangling bond per atom and to stoichiometric nuclei. We assume that the edges of the top facet are rows of Ga or As atoms: this is very likely the case at the first ZB → WZ transition (Fig. 1), and surely in WZ sequences with vertical $\{10\bar{1}0\}$ facets and in ZB sequences with lateral facets composed of alternating {111}-type planes [5]. A given nucleus can still be placed at the edge of the top facet in ZB or WZ position, but this entails major differences (Fig. 4). The edge of the ZB nucleus is the same as that of the top facet, and these two edges develop tilted lateral facets of $\{111\}A$-type at Ga edges [Fig. 4(a); position index $j = A$) or $\{111\}B$-type at As edges [Fig. 4(b); $j = B$]. Conversely, the atoms at the edge of the WZ nucleus differ from those at the edge of the top facet; this generates a vertical lateral facet of $\{10\bar{1}0\}$ WZ type [Fig. 4(c); $j = W$].

Hence, if a given nucleus forms at the triple phase line, the effective areal energy $\tilde{\gamma}_j$ of the portion of its lateral surface in contact with the vapor depends on its position j, for two reasons. First, the lateral facets developed are different. Second, in the two possible ZB positions, these facets are tilted toward ($j = A$) or away from ($j = B$) the wire axis, which modifies the areas of the solid-liquid and liquid-vapor interfaces. This effect can again be estimated by considering simplified geometries. We find $\tilde{\gamma}_j = \gamma_j/\cos\theta_j + (\gamma_{\rm LS} + \gamma_{\rm LV}\cos\beta)\sin\theta_j$, with γ_j the energy of the interface between lateral facet and vapor and θ_j its angle with the vertical (Fig. 4). Our $\tilde{\gamma}_j$ have the same form as the energies calculated by Ross *et al.* for laterally facetted nanowires [20], but they pertain to monolayer-high nuclei. These joint effects transform Eq. (2) into a position-dependent formation enthalpy:

$$\Delta G_j = -\mathrm{Ah}\Delta\mu + \mathrm{Ph}\Gamma_j + A\gamma_{\rm SN} \qquad (3)$$

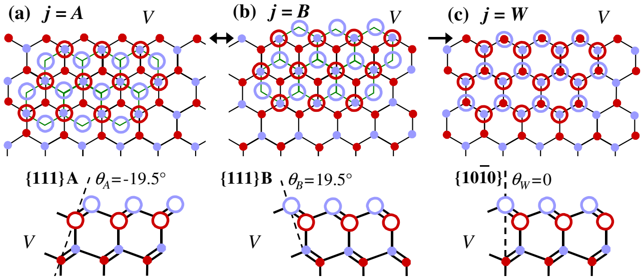

FIG. 4 (color online). Top (top row) and side (bottom row) views of a given nucleus in ZB (a,b) and WZ (c) positions at Ga (a,c) or As (b) edges of the top facet. Edges are indicated by arrows (top), the vapor side by V, and nonvertical dangling bonds by segments (bottom). Key as in Fig. 3.

with $\Gamma_j = (1-\alpha)\gamma_{\ell L} + \alpha(\tilde{\gamma}_j - \gamma_{\mathrm{LV}}\sin\beta)$ and α and P as in Eq. (2). In Eq. (3), only the last two terms differ between nuclei, and the last one cancels in ZB position.

To find simple explicit criteria for ZB formation, we must specify the shape of the nuclei, although this choice is not critical. We opt for equilateral triangles of side D, one of them at the triple phase line ($\alpha = 1/3$). From Eq. (3), we obtain the three formation enthalpies which we maximize with respect to D to obtain the critical size $D_j^\star$ and the energy barrier $\Delta G_j^\star = \Delta G_j(D_j^\star)$ for each nucleus position j:

$$\Delta G_W^\star = \frac{3\sqrt{3}}{2}\frac{h\Gamma_W^2}{\Delta\mu - \frac{\gamma_F}{h}}, \qquad \Delta G_j^\star = \frac{3\sqrt{3}}{2}\frac{h\Gamma_j^2}{\Delta\mu} \quad \text{if } j = A, B \tag{4}$$

with $\Gamma_j = \frac{1}{3}(2\gamma_{\ell L} + \tilde{\gamma}_j - \gamma_{\mathrm{LV}}\sin\beta)$ for $j = A, B, W$. WZ nucleation dominates if $\Delta G_W^\star < \Delta G_j^\star$ for $j = A, B$. This requires two conditions. The first one, $\tilde{\gamma}_W < \tilde{\gamma}_j$ for $j = A$, B, is material-related and involves only interface energies. The second, growth-related, condition is that the supersaturation be larger than a critical value, $\Delta\mu^\star = \max_{j=A,B}(\frac{\Gamma_j^2}{\Gamma_j^2-\Gamma_W^2}\frac{\gamma_F}{h})$, to overcome the stacking fault.

As a first approximation, we estimate the ZB $\tilde{\gamma}_j$ energies from those of $\{111\}$ surfaces (Fig. 4) computed for As-rich (MBE) vapors, namely $\gamma_A = 0.82$ and $\gamma_B = 0.69\ \mathrm{J\cdot m^{-2}}$ [21]. In the extreme cases of drop surfaces of pure Ga and pure Au, this gives respectively $\tilde{\gamma}_A = 0.76$ and $0.83\ \mathrm{J\cdot m^{-2}}$ and $\tilde{\gamma}_B = 0.84$ and $0.77\ \mathrm{J\cdot m^{-2}}$. Although $\tilde{\gamma}_W = \gamma_{10\bar{1}0}$ is unknown, we note that even relatively high values would satisfy the material condition for WZ formation. This hypothesis is strengthened by calculating the critical supersaturations $\Delta\mu^\star$ for a plausible range of such values, e.g., $0.7 \le \tilde{\gamma}_W \le 0.75\ \mathrm{J\cdot m^{-2}}$. For a Ga drop surface with $\beta = 120°$, and taking γ_F as half the stacking fault energy in bulk GaAs [5,22], $\Delta\mu^\star$ ranges between 230 and 1570 meV, which is indeed of the order of our experimental supersaturations (several 100 meV).

In summary, we have developed a nucleation-based model to explain the occurrence of the wurtzite phase in nanowires of zinc blende semiconductors. A key result is that 2D nucleation takes place preferentially at the vapor-liquid-solid triple phase line. We believe that the conditions for this to happen are met in many systems, with consequences going far beyond the particular problem studied here. When formed at the triple phase line, wurtzite and zinc blende nuclei present major differences and wurtzite formation is actually favored for certain ranges of the relevant interface energies. In addition, the supersaturation of the liquid must be high enough, in agreement with our experimental results for GaAs nanowires. Whether these conditions are met has to be checked for each material and growth method.

Our aim was to identify important effects and parameters, not yet to give a complete description of the complex interplay of the two phases. We now intend to calculate the actual nucleation probabilities (including the effects of temperature and geometry), evaluate more precisely the energies of various nuclei (including nonstoichiometric ones) forming on nanowires with different structures and cross-sections, and take into account growth methods and growth conditions in more details, in particular, the supersaturation of each atomic species.

This work was partly supported by the SANDIE Network of Excellence of the European Commission (Contract No. NMP4-CT-2004-500101).

*frank.glas@lpn.cnrs.fr

[1] M. Koguchi, H. Kakibayashi, M. Yasawa, K. Hiruma, and T. Katsuyama, Jpn. J. Appl. Phys. **31**, 2061 (1992).
[2] X. Duan and C.M. Lieber, Adv. Mater. **12**, 298 (2000).
[3] A.I. Persson, M.W. Larsson, S. Stenstrom, B.J. Ohlsson, L. Samuelson, and L.R. Wallenberg, Nat. Mater. **3**, 677 (2004).
[4] J.C. Harmand, G. Patriarche, N. Péré-Laperne, M.-N. Mérat-Combes, L. Travers, and F. Glas, Appl. Phys. Lett. **87**, 203101 (2005).
[5] J. Johansson, L.S. Karlsson, C.P.T. Svensson, T. Mårtensson, B.A. Wacaser, K. Deppert, L. Samuelson, and W. Seifert, Nat. Mater. **5**, 574 (2006).
[6] R.S. Wagner and W.C. Ellis, Appl. Phys. Lett. **4**, 89 (1964).
[7] C.-Y. Yeh, Z.W. Lu, S. Froyen, and A. Zunger, Phys. Rev. B **46**, 10086 (1992).
[8] G.J. Ackland, Rep. Prog. Phys. **64**, 483 (2001).
[9] M.I. McMahon and R.J. Nelmes, Phys. Rev. Lett. **95**, 215505 (2005).
[10] P. Mohan, J. Motohisa, and T. Fukui, Nanotechnology **16**, 2903 (2005).
[11] I.P. Soshnikov, G.E. Cirlin, A.A. Tonkikh, Y.B. Samsonenko, V.G. Dubovskii, V.M. Ustinov, O.M. Gorbenko, D. Litvinov, and D. Gerthsen, Phys. Solid State **47**, 2213 (2005).
[12] R. Leitsmann and F. Bechstedt, J. Appl. Phys. **102**, 063528 (2007).
[13] T. Akiyama, K. Sano, K. Nakamura, and T. Ito, Jpn. J. Appl. Phys. **45**, L275 (2006).
[14] B. Mutaftschiev, R. Kern, and C. Georges, Phys. Lett. **16**, 32 (1965).
[15] E.I. Givargizov, J. Cryst. Growth **31**, 20 (1975).
[16] V.G. Dubrovskii and N.V. Sibirev, Phys. Rev. E **70**, 031604 (2004).
[17] D. Kashchiev, Crystal Growth & Design **6**, 1154 (2006).
[18] D.T. Wu, in *Solid State Physics, vol. 50* (Academic Press, San Diego, 1997), pp. 38–187.
[19] A. Zangwill, *Physics at Surfaces* (Cambridge University Press, Cambridge, 1988).
[20] F.M. Ross, J. Tersoff, and M.C. Reuter, Phys. Rev. Lett. **95**, 146104 (2005).
[21] N. Moll, A. Kley, E. Pehlke, and M. Scheffler, Phys. Rev. B **54**, 8844 (1996).
[22] S. Takeuchi and K. Suzuki, Phys. Status Solidi A **171**, 99 (1999).